Inward-rectifier Potassium Channels in Basolateral Membranes of Frog Skin Epithelium

VALERIE URBACH, EMMY VAN KERKHOVE, and BRIAN J. HARVEY

From the Department of Cellular and Molecular Biology, Commissariat à l'Energie Atomique, Laboratoire Jean Maetz BP68, F-06230 Villefranche-sur-mer. France; and Cellular Physiology Research Unit, Department of Physiology, University College, Cork, Ireland

ABSTRACT Inward-rectifier K channel: using macroscopic voltage clamp and single-channel patch clamp techniques we have identified the K^+ channel responsible for potassium recycling across basolateral membranes (BLM) of principal cells in intact epithelia isolated from frog skin. The spontaneously active K^+ channel is an inward rectifier (K_{ir}) and is the major component of macroscopic conductance of intact cells. The current–voltage relationship of BLM in intact cells of isolated epithelia, mounted in miniature Ussing chambers (bathed on apical and basolateral sides in normal amphibian Ringer solution), showed pronounced inward rectification which was K^+-dependent and inhibited by Ba^{2+}, H^+, and quinidine. A 15-pS K_{ir} channel was the only type of K^+-selective channel found in BLM in cell-attached membrane patches bathed in physiological solutions. Although the channel behaves as an inward rectifier, it conducts outward current (K^+ exit from the cell) with a very high open probability (P_o = 0.74–1.0) at membrane potentials less negative than the Nernst potential for K^+. The K_{ir} channel was transformed to a pure inward rectifier (no outward current) in cell-attached membranes when the patch pipette contained 120 mM KCl Ringer solution (normal NaCl Ringer in bath). Inward rectification is caused by Mg^{2+} block of outward current and the single-channel current–voltage relation was linear when Mg^{2+} was removed from the cytosolic side. Whole-cell current–voltage relations of isolated principal cells were also inwardly rectified. Power density spectra of ensemble current noise could be fit by a single Lorentzian function, which displayed a K dependence indicative of spontaneously fluctuating K_{ir} channels. Conclusions: under physiological ionic gradients, a 15-pS inward-rectifier K^+ channel generates the resting BLM conductance in principal cells and recycles potassium in parallel with the Na^+/K^+ ATPase pump.

INTRODUCTION

Sodium absorption across tight-junction epithelia occurs by passive entry into the cell at the apical membrane through amiloride-blockable channels and active secretion

Dr. Van Kerkhove's present address is Department of Physiology, Limburgs Universitair Centrum, B-3590 Diepenbeek, Belgium.

Address correspondence to Dr. B. J. Harvey, Cellular Physiology Research Unit, Department of Physiology, University College, Cork, Ireland.

J. GEN. PHYSIOL. © The Rockefeller University Press · 0022-1295/94/04/0583/22 $2.00
Volume 103 April 1994 583–604

across the basolateral membrane via an Na^+/K^+ ATPase pump. Potassium is recycled across this membrane through a channel. In the Ussing model the basolateral membrane behaves like a pure potassium electrode in that the variations in transepithelial potential in response to changes in extracellular K^+ concentration can be predicted from the Nernst equation (Koefoed-Johnsen and Ussing, 1958). This could imply that one type of K^+ channel, possibly showing Goldman rectification, is involved in recycling potassium. In absorptive epithelia, however, where K^+-dependent current–voltage relations have been reported, it seems that the K^+-conductive pathway at the basolateral membrane cannot be described by Goldman-Hodgkin-Katz (GHK) formalism but instead shows a higher conductance for inward than for outward current (inward rectification) (Nagel, 1985; Horisberger and Giebisch, 1988). Similar conclusions that an inward-rectifier K^+ (K_{ir}) channel dominates the membrane conductance was reached in recent patch clamp studies in isolated cells from frog skin (García-Díaz, 1991).

The isolated frog skin is the classical model for sodium-absorbing tight epithelia, but little is known about the physiology of the potassium channel(s) in the basolateral membrane of this tissue. Our specific aim in this study was to identify the type of K^+ channel in basolateral membranes responsible for steady-state K^+ recycling and compare the single-channel and macroscopic K^+ conductance properties in the intact epithelium.

This is the first investigation of single K^+ channels in basolateral membranes of an intact sodium-transporting epithelium. The combination of the patch clamp recording of single-channel activity and conventional microelectrode measurements of membrane potential and conductance in the intact epithelium permits a detailed analysis of K^+ channel physiology. The data reported here show that the macroscopic inward rectification of basolateral membrane current is generated by inward-rectifier K^+ channels which share similar voltage-gated properties with the anomalous rectifier of excitable cells (Hagiwara, 1983).

METHODS

Epithelium Isolation

Intact epithelial sheets were isolated from the ventral skin of *Rana esculenta* by means of a combined enzymatic and mechanical separation technique. The isolated skin (11 cm^2) was exposed on the corial side for 60 min to 1 mg/ml collagenase (125 IU activity; Worthington Biochemical Corp., Freehold, NJ) under 10 cm of hydrostatic pressure at 30°C. This treatment was terminated when blisters first formed on the epithelial side. A fine polythene catheter (0.25 mm o.d.) was introduced into a blister and Ringer solution was injected into the subepithelial space. This resulted in detachment of a large sheet of epithelium (7 cm^2). The basement membrane could easily be detached by flushing the epithelium in calcium-free Ringer buffered with 2 mM EGTA for 3–10 min. Epithelia isolated in this way had transepithelial sodium transport rates and transepithelial resistances comparable with whole skins. The epithelium was mounted basolateral side upwards in a miniature Ussing chamber which allowed conventional short-circuit current measurements, intracellular microelectrode recording, and single-channel patch clamp studies to be performed on the same epithelium (Fig. 1).

The frog skin epithelium is a complex three- to five-cell layered structure composed of several cell types that include granular cells and mitochondria-rich cells in the layers

immediately below the outermost layer of dead cells (stratum corneum), and germinal cells in the deeper layers. There is a great deal of evidence from studies of cell volume and membrane potential responses to amiloride, ouabain and changing external Na and K concentrations that the multilayered epithelium acts as a syncytial Na transport compartment (Kristensen and Ussing, 1985; Rick, Dorge, von Arnim, and Thurau, 1978). Only the first granular cell layer has a polarized apical membrane containing Na^+ channels and are termed principal cells. The cells in deeper layers are coupled to the first reactive cell layer by gap junctions (Farquhar and Palade, 1965; Sharin and Blankemeyer, 1989) so that they share the sodium transport pool. The mitochondria-rich cells, which are the site of active acid secretion, are not considered to be part of this syncytium. In our isolated epithelial preparation, principal and mitochondria-rich cells could easily be distinguished and although we also found inward-rectifier K^+ channels in the basolateral membranes of mitochondria-rich cells, only the properties of K_{ir} channel in principal cells are reported here.

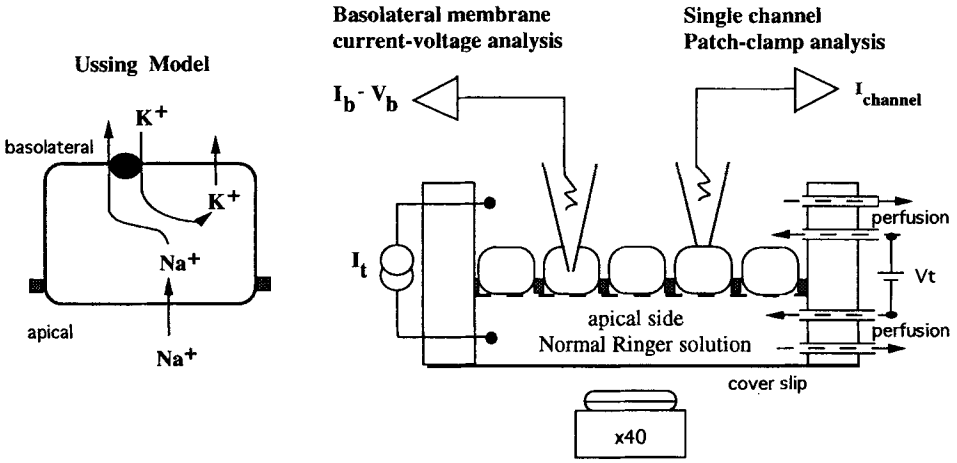

FIGURE 1. The Ussing model of sodium reabsorption through principal cells and schema of the experimental arrangement for recording short-circuit current, intracellular potential, and single-channel activity in an isolated epithelium mounted in a miniature Ussing chamber on the stage of an inverted Nikon Diavert microscope.

The experiments were carried out at room temperature. The apical side was always bathed in standard NaCl Ringer solution and the basolateral side was continually superfused in either Na or K Ringer solutions of composition shown in Table I. In solutions containing EGTA, free concentrations of calcium were calculated using a computer program (Chang, Hsieh, and Dawson, 1988). All chemicals were purchased from Sigma Chemical Co. (St. Louis, MO).

Dissociated Cells

Single cells were isolated for whole-cell patch clamp recording. The basolateral side of the epithelium mounted in an Ussing chamber was superfused in Ca-free Ringer solution containing 10 mM EGTA for 2–5 min. A small area of epithelium was then scraped with a broken tip patch electrode to detach single cells from the epithelial sheet. In this way cells could be isolated from every layer of the epithelium. The combination of scraping and suction of cells was also used to expose basolateral membranes of the cells in the outermost layer ("first

reactive principal cell layer") for single-channel recording. These cells have polarized apical and basolateral membranes separated by tight junctions whereas cells from deeper layers are nonpolar and behave electrically as a single basolateral membrane.

Basolateral Membrane Current–Voltage Analysis

Conventional microelectrodes were prepared from borosilicate glass capillaries (250F Clark Electromedical, Pangbourne, UK) using a programmable puller (DMZ Universal Puller, Werner Zeitz, Augsburg, Germany). Electrode tip resistance was between 40 and 60 MΩ when filled with 1 M KCl solution. The electrical arrangement for recording basolateral membrane current–voltage ($I_b - V_b$) relations has been previously described in detail (Harvey, Thomas, and Ehrenfeld, 1988). After microelectrode impalement of principal cells from the basolateral side a transepithelial bipolar pulse train (pulse duration 210 ms, interval 100 ms) incrementing in 5-mV steps to ±200 mV was generated under computer command via a voltage clamp

TABLE I

Composition of Saline Solutions Used in Bath and Patch Pipette

	NaCl	KCl*	$MgCl_2$	$CaCl_2$	HEPES	EGTA	pH*
				mM			
Extracellular solutions							
Na Ringer	110	3.7	1	2	6	—	7.4
K_{ext} pCa 3	—	107	1	1	10	—	7.4
Intracellular solutions							
K_{int} pCa 7	—	107	1.15	5.92	10	10	7.4

Whole-Cell Pipette Solutions

Kgluc	KCl	$MgCl_2$	$CaCl_2$	NaAc	NaPyr	Asp	GTPγS	EGTA	HEPES	pH
					mM					
100	20	1.22	2.96 (pCa8)	3	5	5	0.01	5	10	7.4

Abbreviations: Kgluc; potassium gluconate; NaAc, sodium acetate; NaPyr, sodium pyruvate; Asp, aspartic acid.

*The pH of K_{int} solutions was adjusted with KOH which increased the K^+ concentration to 120 mM. In potassium gluconate solutions Ca activity is reduced by 90% due to a chelating effect of gluconate (measured with a Ca-selective macroelectrode). This was compensated for in the calculation of free calcium.

amplifier (model VCC600, Physiologic Devices, Houston, TX). The basolateral membrane potential was measured with a high input impedance differential amplifier (model 750, World Precision Instruments Inc., Hew Haven, CT). Voltage and current outputs were digitized and stored on computer for analysis. Barium-sensitive current–voltage relations were obtained by subtracting $I_b - V_b$ relations recorded in the absence and presence of 5 mM $BaCl_2$. The K^+ selectivity of the basolateral membrane conductance was examined by running voltage clamp ramps in standard Ringer (3.7 mM K^+) solution and in Ringer with 37 mM K^+ added as gluconate salt. Transference numbers for potassium (T_K) were calculated from the magnitude of V_b changes in response to varying E_K by 58 mV (increasing external [K] from 3.7 to 37 mM).

Single-Channel Recording

The cell-attached and inside-out configurations of the patch-clamp technique (Hamill, Marty, Neher, Sakmann, and Sigworth, 1981) were used for single channel studies. Patch pipettes (tip

resistance 4–10 MΩ) were prepared from borosilicate glass capillaries (Vitrex, Modulohm, Herlev, Denmark), pulled, and polished on a programmable puller (DMZ, Zeitz Instrumente, Augsburg, Germany). The patch pipettes were filled with either standard NaCl Ringer or an intracellular-like K^+ solution ("K_{int}" composition given in Table I). All solutions were filtered through 0.2-μm cellulose disks (Millipore Corp., Bedford, MA). Current and voltage recordings from patch-clamp electrodes were amplified (Biologic RK 300 patch-clamp amplifier, Biologic, Claise, France), passed through a 30-kHz filter and stored on video tape (Betamax, Sony, Tokyo, Japan) after pulse code modulation (PCM model 501ES, Sony). The single-channel current records were digitized and displayed in real time using a digital oscilloscope (model 310, Nicolet Instrument Corp., Madison, WI). Single-channel current records for illustrations were filtered at 1 kHz using a Tchebycheff filter and replayed on a chart recorder (model RS3200, Gould Instruments, Valley View, OH).

Current and voltage signals were digitized using a 16-bit A/D converter (CED 1401, Cambridge Electronic Design, Cambridge, UK) after low-pass (−3 dB) filtering at 5 kHz (8 pole Bessel filter, model 902, Frequency Devices Inc., Haverhill, MA) and analysed with a model 80486 50-MHz Dell Corp. (Limerick, Ireland). Steady-state current–voltage relations were run and analyzed using VGEN and PAT programs (J. Dempster, Strathclyde Electrophysiology Software version 6.1, University of Strathclyde, Scotland) and instantaneous current–voltage trials were generated using PULSESTIM and VCLAMP programs (Cambridge Electronic Design, release EPC 5.0). Single-channel current amplitude histograms, open probability, and open and closed dwell times were analyzed from data segments of 20–60-s duration using the PAT program. Single-channel K^+ permeability was calculated from the general form of the GHK equation:

$$I = \frac{P_K \cdot V \cdot F^2}{RT} \cdot \frac{\{[K]_i \exp(VF/RT) - [K]_o\}}{\{\exp(VF/RT) - 1\}} \quad (1)$$

where R, T, and F have their usual meanings, $[K]_o$ and $[K]_i$ are the external and internal concentrations of potassium, and P_K is the permeability to K^+. Cation movement across the membrane from the external to the cytoplasmic side is defined as inward current and shown as downward deflections in single-channel records.

Whole-Cell Current–Voltage Analysis in Isolated Cells

The whole-cell configuration was obtained from the cell-attached mode after breaking the membrane patch by applying a brief negative pressure pulse (−200 mbar) in the pipette. Whole-cell currents were amplified (RK300 Biologic), digitized at 20 kHz (CED 1401) and sampled in real time on hard disk at an acquisition rate of 5 kHz. Current–voltage relations were analyzed using CED VCLAMP software.

Whole-Cell Current Noise Analysis

The application of current noise analysis to epithelial cells has been reviewed in detail by Van Driessche and Zeiske (1985) and we give only the essentials of the technique as applied in this study. Current noise was recorded from isolated dispersed single principal cells perfused through the patch pipette with an intracellular-like K^+ solutions ("whole-cell" solution in Table I). Whole-cell current fluctuations were amplified by the patch clamp amplifier and split into low and high pass components using Bessel filters with cutoff frequencies at 1 kHz and 0.1 Hz, respectively, and stored on video tape. The current noise signal was replayed through the CED1401 A/D converter, digitized at 5 kHz, and analyzed by a fast Fourier transform using customized software. The variance of the fluctuations in current noise is presented as a function of the alternating current frequencies contained in the current noise (power density spectra).

An average power spectrum was compiled from 200 record segments (each of 250 ms in duration) and channel noise was recorded at pipette holding potentials between ±100 mV relative to E_K. A Lorentzian curve was fitted to the power spectrum using a Levenberg-Marquadt iterative fitting algorithm (K. Brown, University of Cincinatti). For a channel that fluctuates between distinct open and closed states, the power spectrum will contain a Lorentzian defined by the equation:

$$L(f) = S_o/(1 + (f/f_c)^2) \tag{2}$$

where S_o is the low frequency assymptote or plateau value and f_c the corner or cutoff frequency at which the spectral power is $S_o/2$. The cutoff frequency is related to the time constant (t) of channel open/closure fluctuations by

$$t = (2\Pi \cdot f_c)^{-1} \tag{3}$$

where $t = (\alpha + \beta)^{-1}$ and α and β are on- and off-rates for channel transitions from open to closed and closed to open states, respectively, based on a two-state model, OPEN $\underset{\beta}{\overset{\alpha}{\rightleftharpoons}}$ CLOSED. The time constant is related to open probability by

$$P_o = \beta/(\alpha + \beta) \tag{4}$$

Closed and open transition rates were calculated from

$$\beta = P_o \cdot 2 \cdot \Pi \cdot f_c, \qquad \alpha = (2 \cdot \Pi \cdot f_c) - \beta \tag{5}$$

using values for open probabilities (P_o) determined in excised inside-out recordings under identical bathing conditions and voltage. The open and closed rate constants α^{-1} and β^{-1} were compared with time constants t_o and t_c measured from the exponential distribution of open and closed times, respectively. The variance in channel current-noise (σ^2) was calculated by integrating the power spectrum

$$\sigma^2 = (\Pi \cdot f_c \cdot S_o)/2 \tag{6}$$

and the single-channel conductance (G_s) was then determined from

$$G_s = \sigma^2/[I_m(V_p - E_K)] \tag{7}$$

where I_m is the mean direct current recorded in the power spectrum and V_p is the pipette holding voltage. Single-channel current (I_s) can then be obtained from

$$I_s = G_s(V_p - E_K) \tag{8}$$

The density of channels in the cell membrane (N) was estimated from

$$N = \Pi \cdot f_c \cdot S_o/2(I_s)^2 \cdot P_o \cdot (1 - P_o) \tag{9}$$

Data are presented as mean values ± SEM.

RESULTS

Macroscopic Properties of Basolateral Membrane Conductance

The basolateral membrane current–voltage relationship ($I_b - V_b$) shows steep inward rectification under spontaneous Na^+ transport conditions (Fig. 2 *A*). The membrane is therefore more conductive for inwardly directed current (cation entering or anion leaving the cell) than for outward current (cation leaving or anion entering the cell). The degree of rectification and the potential at which the current changes sign

(reversal potential, V_r) were a function of the serosal K^+ concentration. Raising $[K^+]$ in the serosal bath from 3.7 to 37 mM produced an increase in conductance for inward current which was 10-fold greater than for outward current and shifted V_r by +48 mV. These effects are expected if the basolateral membrane current is carried mainly by potassium. Practically all types of K^+ channels are blocked by barium ions and the experiment in Fig. 2 *A* shows that addition of 5 mM $BaCl_2$ to the serosal bath completely eliminated the inward current rectification. Ba^{2+} reduced the potassium transference from 0.82 ± 0.05 to 0.09 ± 0.03 (n = 10 cells) and the membrane potential no longer responded to changes in external K^+. The K^+-specific current–voltage relations of the basolateral cell membranes was extracted by taking the difference between $I_b - V_b$ curves measured in control and in the presence of barium (Fig. 2 *B*). Ba^{2+}-sensitive $I_b - V_b$ relations show strong inward rectification and the increased membrane conductance for inward current is evident at hyperpolarized membrane potentials. Acidification of the epithelium at pH 6.5 produced a similar decrease in basolateral membrane conductance as in Ba^{2+} (Fig. 3 *A*). Quinidine at

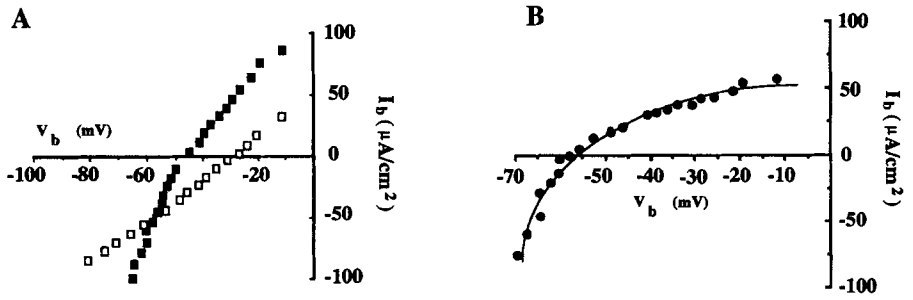

FIGURE 2. Macroscopic current–voltage relations of basolateral cell membranes of isolated frog skin epithelium. (*A*) Control situation: standard Na Ringer solution (■) and after addition of 5 mM $BaCl_2$ (□). (*B*) "Difference" or Ba^{2+}-sensitive current–voltage relation for *A*.

high concentrations (100 μM) also inhibited the inward rectification of basolateral membrane current (Fig. 3 *B*). Quinidine has been used to block Ca^{2+}-activated K^+ currents in turtle colon (Chang and Dawson, 1988) but other inhibitors of these classes of K^+ channels were without effect on membrane conductance. For example, $I_b - V_b$ relations were insensitive to quartenary amononium ions such as (5 mM) tetraethyl ammonium (Fig. 3 *C*), tetrapentyl ammonium, or choline. The honey bee venom, apamin, which is considered specific for calcium-dependent "small" conductance K^+ channels, had no effect (at 10^{-9} M) on basolateral membrane current. The maxi-K channel blocker, charybdotoxin (10^{-8} M) was also without effect, making it unlikely that the basolateral membrane K^+ conductance is generated by calcium-activated K^+ channels. Basolateral membrane current was, however, sensitive to removal of extracellular Ca^{2+} which enhanced inward rectification (Fig. 3 *D*).

Single-Channel Recording

Cell-attached recordings in NaCl Ringer solution. We found it relatively easy to obtain patch-clamp seal resistances >10 GΩ on basolateral cell membranes of principal

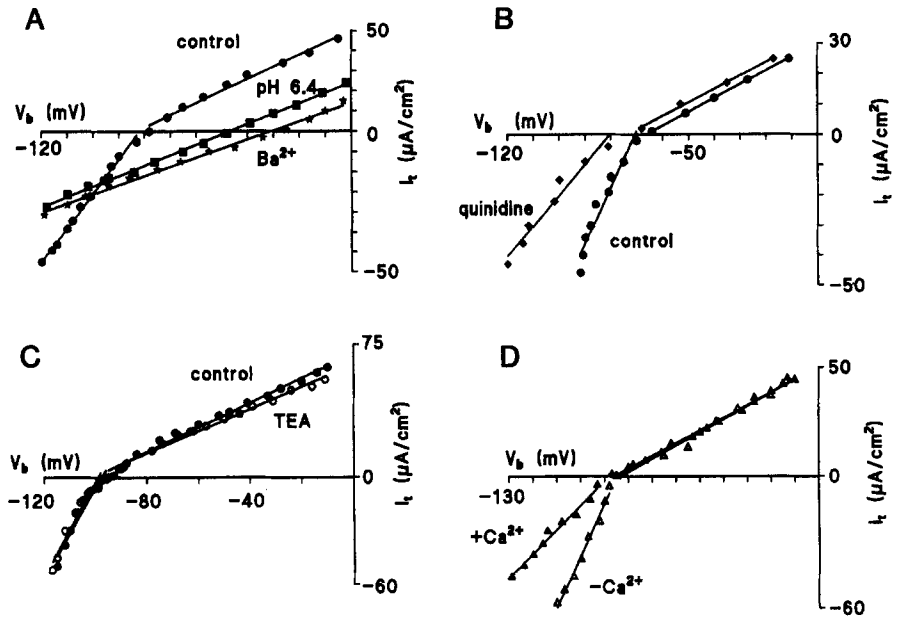

FIGURE 3. Current–voltage relations for basolateral cell membranes. (*A*) Effect of intracellular acidification from a control pH 7.4 (●) to pH 6.4 (■) and comparison with effects of 5 mM $BaCl_2$ (★). (*B*) Effect of quinidine 100 μM: control (●); quinidine (◆). (*C*) Effect of tetraethylammonium (TEA) 5 mM: control (●); TEA (○). (*D*) Effect of removing Ca^{2+} from basolateral Ringer solution, control (▲), calcium-free (△).

cells, but almost 50% of basolateral membrane patches showed no channel activity. When the experiments were made with sodium Ringer solution in the bath and patch pipette, only one type of K^+-selective channel was found in over 500 cell-attached patches in normal Na-transporting epithelia. The spontaneously active K^+ channels showed properties of inward rectification which was similar to the voltage dependence of the macroscopic basolateral membrane current. The single-channel current–voltage relationship (Fig. 4) is opposite to that expected from GHK formalism.

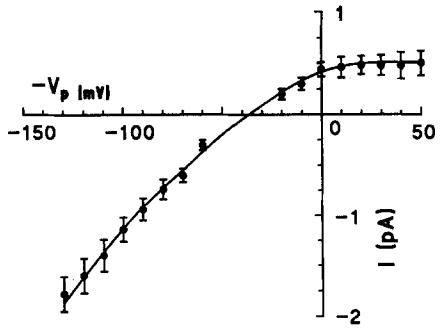

FIGURE 4. Single-channel current–voltage relationship of K_{ir} channel in cell-attached basolateral membranes exposed to normal Ringer solution (n = 8 cells). Single-channel currents were sampled at the clamped voltage from 10 record segments each of 20-s duration and filtered at 1 KHz. The imposed membrane voltage is shown with pipette solution as reference ($-V_p$). The true reversal potential (V_r) equals the sum of membrane potential (−50 mV) and the pipette holding potential at which current changes sign ($-V_p$ = −45 mV). V_r agrees with estimates of E_K (−95 mV). The single-channel current–voltage relationship shows opposite (anomolous) rectification predicted from GHK formalism.

Despite the favorable chemical gradient for K^+ exit from the cell into the bath (and patch pipette), the channel behaves as an inward rectifier, being more conductive for inward current than for outward current. The unit current amplitude was small (0.5 pA) at the resting membrane potential and a slope conductance of 3pS was calculated from the current–voltage relation at zero holding potential. When the potential across the patch was hyperpolarized by >40 mV the single-channel current reversed direction. As expected for a K^+-selective channel, the reversal potential ($V_r = E_m - V_p$) at which the current changes sign agrees with reasonable measurements of the Nernst potential for K^+ ($[K^+]_i$ = 120 mM, E_K = −88 mV, E_m = −50 mV, and V_p = 40 mV) (Harvey and Kernan,1984). At V_p > 40 mV the electrochemical driving force favors K^+ entry from the bath (and pipette) into the cell. A mean single-channel conductance (Eq. 8) of 15 ± 2 pS (n = 8 cells) was calculated between the reversal potential and V_p = 100 mV.

The experiment in Fig. 5 *A* shows single-channel current recordings from an inward-rectifier K^+ channel (K_{ir}) in the basolateral membrane of a principal cell in the cell-attached mode when both the bath and pipette contained normal NaCl Ringer solution. At the depolarized membrane potential (V_p = −30 mV), the channel was open and passed outward current for practically the whole duration of the recording. When the membrane potential was hyperpolarized (V_p > 40 mV), the channel conducted inward current and openings occurred in bursts with rapid transitions to the closed state during the burst. Channel activity often reflected the openings of multiple ion channels in the patch and was measured as the product of the number of active channels and open probability ($N{\cdot}P_o$). Channel activity was calculated from

$$N{\cdot}P_o = \Sigma(n{\cdot}t_n) \tag{10}$$

where n represents the channel state, 0 = closed, 1 = one channel open, 2 = two channels open, etc., and t_n is the duration of state n. Channel activity is shown as a function of applied voltage in Fig. 5 *B*, and was near-maximal at the resting membrane potential and decreased for inward K^+ current when the membrane voltage was hyperpolarized beyond E_K. These results show that the K_{ir} channel can conduct K^+ out of the cell with a very high open probability. An evaluation of how the K_{ir} channel could influence the macroscopic basolateral membrane conductance can be obtained from the voltage dependence of the product of single-channel current and channel activity ($I{\cdot}N{\cdot}P_o$) as shown in Fig. 5 *C*. K_{ir} channel activity will confer inward rectification properties on the basolateral membrane, and behaves as a near-constant current source for outward current. This would appear to be an ideal property for a channel recycling K^+ in parallel with a constant current Na/K pump.

Cell-attached recordings with KCl in the patch pipette. In cell-attached patches bathed with 125 mM KCl solution in the pipette and NaCl Ringer solution in the bath, >75% of patches showed spontaneous K^+-selective channel activity. Similar K_{ir} channel activity was recorded in K_{ext} (1 mM Ca^{2+}) or in K_{int} pipette solutions (100 mM Ca^{2+}) but the latter solution was used preferentially to allow transfer from cell-attached to whole-cell recording configurations in the same cell. The experiment in Fig. 6 *A* shows single-channel currents recorded when pipette voltage was varied between ±100 mV in 10-mV steps with K_{int} in the pipette and normal Ringer in the

bath. The channel conducted K^+ from pipette into the cell at hyperpolarized membrane potentials but outward currents were barely detectable even when the membrane was depolarized by 100 mV. The corresponding current–voltage relationship is included in Fig. 6 *B*. Single-channel conductance measured between V_p −20 and +100 mV was 35 ± 4 pS (n = 12). In the presence of high external K^+ the

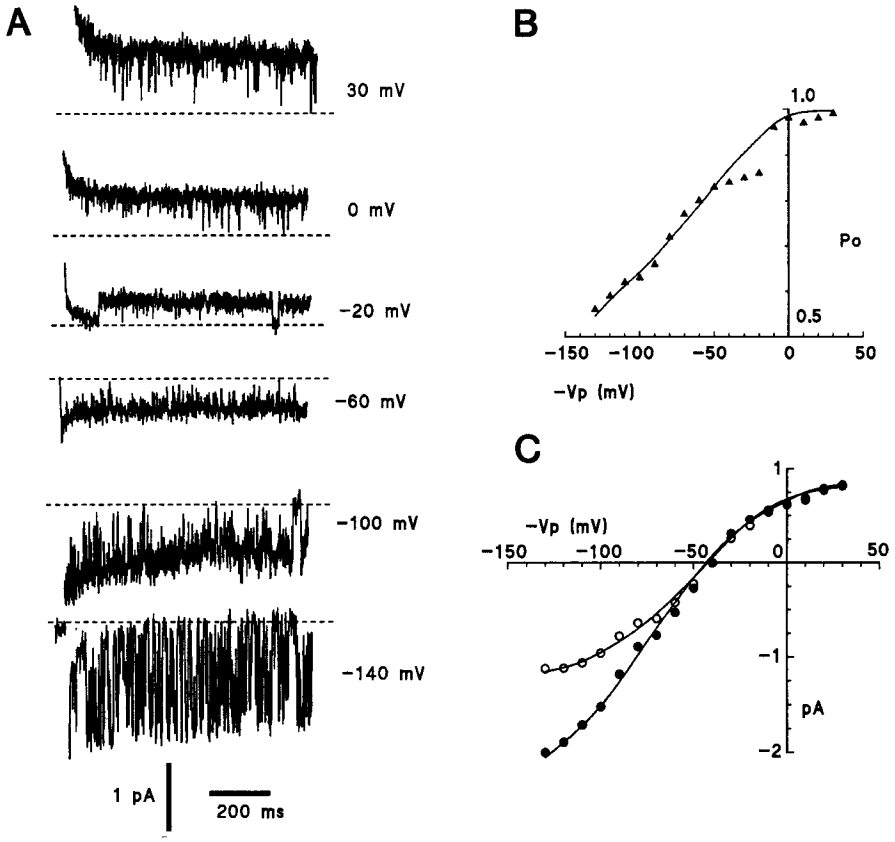

FIGURE 5. (*A*) Single-channel recording of K_{ir} channels in cell-attached basolateral membranes, at various pipette voltages ($-V_p$ shown at edge of trace) in cells exposed to normal sodium Ringers in bath and patch pipette. The dashed line indicates the closed level. Outward currents are upward and Inward currents appear as downward rapid fluctuations. (*B*) Voltage dependence of K_{ir} channel activity ($N \cdot P_o$). (*C*) The contribution of K_{ir} channel activity to the macroscopic basolateral membrane current–voltage relation can be evaluated from the voltage dependence of the product of channel activity and single-channel current ($I \cdot N \cdot P_o$) (mean values for eight cells). The voltage dependence of single channel current alone (●) can be compared with the voltage-dependence of $I \cdot N \cdot P_o$ (○).

channel is transformed to an almost pure inward rectifier and only movement of K^+ into the cell is possible. The voltage dependence of channel activity ($N \cdot P_o$) recorded from a multichannel patch clearly shows this diodelike property (Fig. 6 *C*). Channel activity increased with membrane hyperpolarization and this is in contrast to channel behavior observed with standard Na Ringer solution in the pipette where P_o

decreased with membrane hyperpolarization. The open probability for inward current was higher in low calcium pipette solutions compared to high calcium solutions, with Ca^{2+} producing a flicker-type block of inward current openings (not shown). The blocking effect of extracellular calcium was also noted for macroscopic

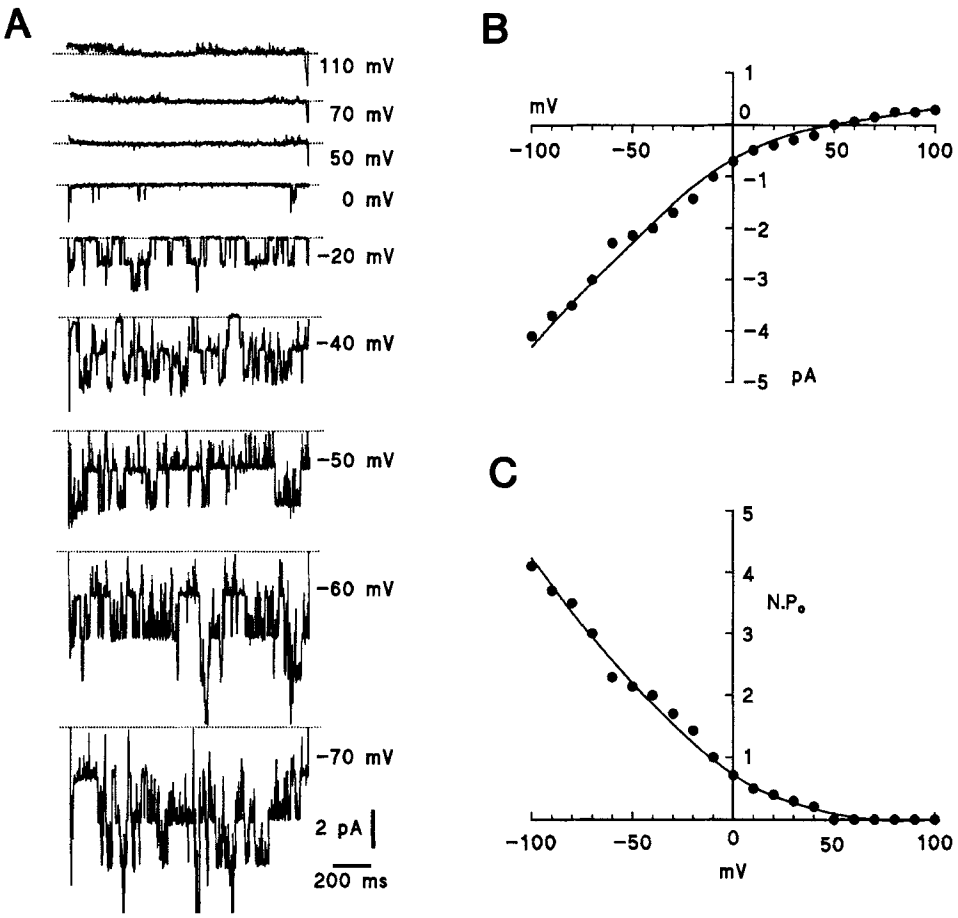

FIGURE 6. Electrical properties of inward-rectifier K^+ channels in cell-attached membranes bathed in standard Na Ringer in bath and Kint solution in the patch pipette. (*A*) Basolateral membrane cell-attached recording of K_{ir} single-channel currents at pipette voltages between ±100 mV. Cutoff frequency 1 kHz. Note absence of outward currents at depolarized membrane potentials. (*B*) Current–voltage relationship of single K^+ channels for conditions in *A*, the channel behaves as a pure inward rectifier. (*C*) Voltage dependence of K_{ir} channel activity for conditions in *A* (mean values for eight cells). The voltage dependence of channel activity is opposite to that observed when standard Na Ringer was used as pipette filling solution.

inward current (Fig. 3 *D*). The single-channel current–voltage relation was practically linear for inward current in high K pipette solutions. Fitting the GHK equation to the current–voltage data between V_p 0 and 100 mV yielded a mean value for the potassium permeability = 0.38 (±0.08)·10^{-13} cm/s (n = 12).

Single-Channel Biophysics in Excised Inside-out Membranes

Na Ringer in the pipette. In excised inside-out membrane patches, the K_{ir} channel conserved the basic properties of inward rectification observed in the cell-attached configuration. The patches were normally excised into intracellular-like KCl Ringer solution (K_{int} at pCa 7, pH 7.2). Single K_{ir} channel currents recorded over a wide voltage range are shown in Fig. 7 *A* from an excised patch exposed to a K_{int} solution on the cytosolic side and standard Na Ringer in the pipette. The membrane was voltage clamped for 800 ms to the potentials (V_c) indicated on the right of the trace.

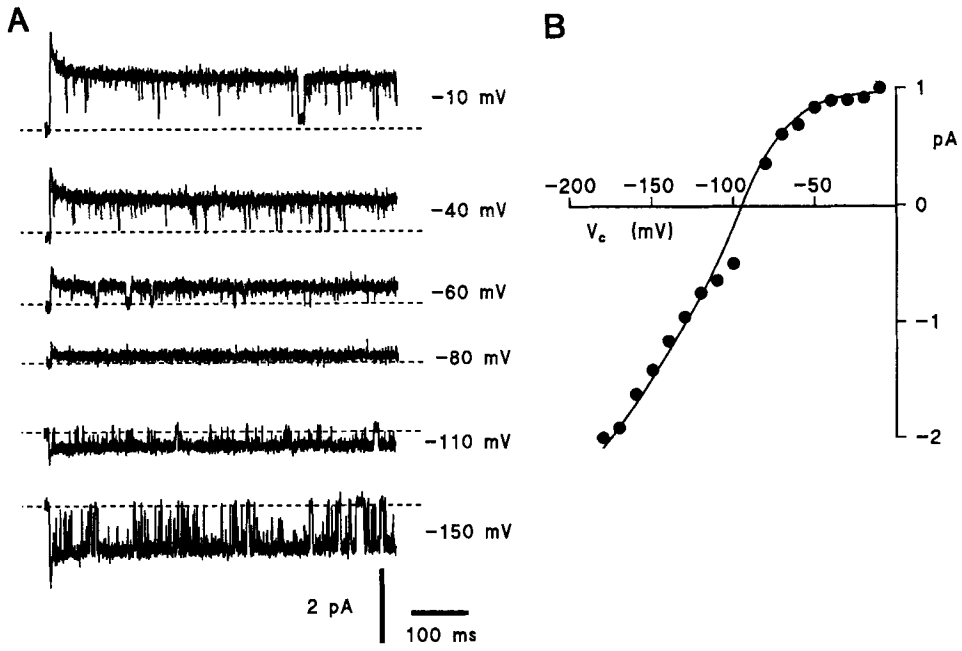

FIGURE 7. Current–voltage relationship of K_{ir} channels in excised inside-out basolateral membranes exposed to standard Na Ringer in the patch pipette and K_{int} solution in the bath. (*A*) Single-channel recording at imposed membrane potentials. The patch potential is shown on the left of each current trace and the closed level is indicated by a dashed line. Cutoff frequency 1 kHz. (*B*) Mean single-channel current–voltage relationship (n = 8) showing inward rectification and reversal potential of −85 mV, which is close to E_K (−88 mV).

The calculated E_K across the patch is −85 mV and it can be seen in Fig. 7 *A* that the channel passes outward current (from bath into pipette) for V_c less negative than E_K and inward current for V_c more negative than E_K. Under these physiological ionic gradients, the reversal potential is close to E_K, indicating a high selectivity for potassium. The mean single-channel current–voltage relationship is shown for eight inside-out patches in Fig. 7 *B* and presents clear inward rectification. The slope conductance for inward current (17 ± 2 pS, n = 18 cells) and for outward current (5 ± 2 pS, n = 18 cells) correspond to the conductances measured in the cell-attached mode. The high open probability for outward current and the flickery-type

openings during inward current are also comparable with the cell-attached observations. The relative permeability of Na^+ to K^+ (P_{Na}/P_K) was obtained in mixed solutions of Na and K from

$$V_r = \frac{RT}{F} \cdot \ln \frac{[K]_o + (P_{Na}/P_K\,[Na]_o)}{[K]_i + (P_{Na}/P_K\,[Na]_i)} \tag{11}$$

where $[K]_o$, $[Na]_o$ are the concentrations (in mM) of external (patch pipette) K^+ (3.7) and Na^+ (120), and $[K]_i$ and $[Na]_i$ are the internal (bath) K^+ (120) and Na^+ (12) concentrations, respectively. P_{Na} and P_K are the permeability to Na^+ and K^+, respectively. The reversal potential (V_r) = -79 ± 0.6 mV ($n = 7$ patches) and the

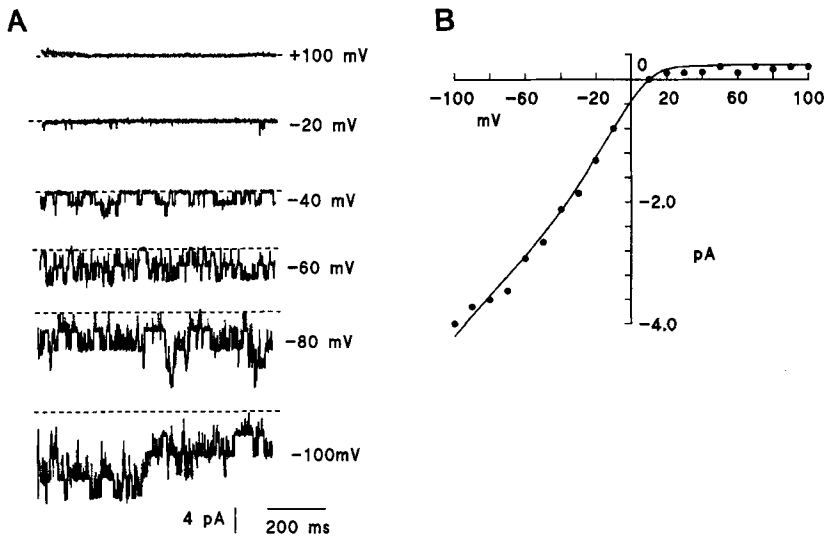

FIGURE 8. Voltage dependence of K_{ir} channel current in excised inside-out basolateral membranes exposed to K_{int} solution on both sides. (*A*) Single-channel recording as a function of imposed membrane voltage. Values of V_c are shown on right of trace, and the closed level is indicated by a dashed line. Note absence of channel opening at depolarized membrane potentials and multiple-channel activity during hyperpolarization. Cutoff frequency 1 kHz. (*B*) Single K_{ir} channel current–voltage relationship showing diode-like behavior. Line through data points fitted by eye (mean values for eight cells).

mean calculated $P_{Na}/P_K = 0.013$, indicating the channel is 77 times more selective for potassium.

Channel activity in symmetrical KCl solutions. In inside-out patches bathed in symmetrical K_{int} Ringer solutions, no outward currents were recorded between 0 and +100 mV relative to E_K (0 mV), whereas the channel was activated at V_c more negative than E_K. Representative single-channel recordings are shown as a function of membrane potential (±100 mV) in Fig. 8 *A* and the current–voltage relationship from a mean of eight cells is given in Fig. 8 *B*. The channel was inactive at depolarized potentials whereas channel activity ($N \cdot P_o$) was greatly increased by membrane hyperpolarization. Since the current–voltage relation presents an ohmic

conductance at hyperpolarized membrane potentials, an estimate of the single-channel K^+ permeability for inward current was calculated from the general form of the GHK equation. The potassium permeability was $0.41 \cdot 10^{-13}$ cm/s, which is in excellent agreement with P_K calculated in cell-attached patches.

Cytosolic Mg^{2+} and inward rectification. Removing magnesium ions from the internal side of inside-out patches, resulted in a loss of inward rectification (Fig. 9 *A*). Single K_{ir} channels displayed near linear current–voltage relations when exposed to Mg-free (2 mM EDTA) symmetrical K_{int} solutions (Fig. 9 *B*). The mean single-channel conductance was 35 ± 2 pS (n = 6 patches) over the membrane potential range ± 100 mV.

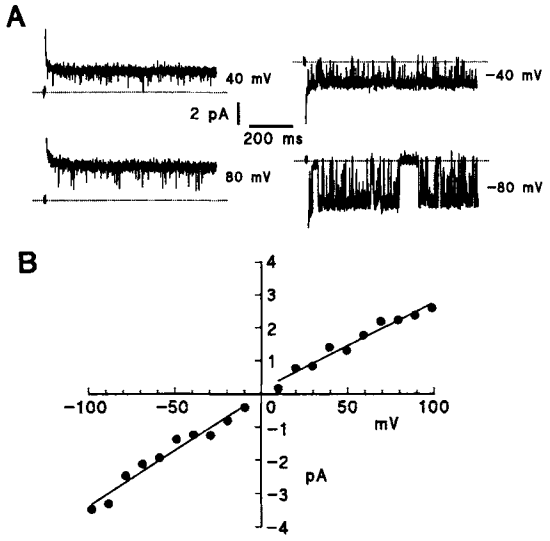

FIGURE 9. (*A*) Recording of K_{ir} channel activity in excised inside-out basolateral membranes exposed to K_{int} solutions on both sides and in the absence of Mg ions from the cytosolic side (2 mM EDTA). (*B*) In Mg-free solutions the single channel current–voltage relation is ohmic in contrast to the pure inward-rectification observed under similar conditions in the presence of 2 mM $MgCl_2$ (Fig. 8).

Inhibition of K_{ir} Channels

The effects of barium were tested on excised inside-out patches bathed in normal Ringer and K_{int} solutions on extra- and intracellular sides, respectively. Barium (5 mM) added to the cytosolic side reduced K_{ir} channel activity instantaneously and reversibly without affecting the open-state conductance. The effects of Ba^{2+} on channel kinetics were voltage-dependent and the reduction in P_o was greater for outward current. Barium reduced P_o for inward current from 0.74 ± 0.04 to 0.28 ± 0.03 and outward current P_o from 0.85 ± 0.04 to 0.02 ± 0.01 (n = 8 cells). Inhibitors of calcium-dependent K^+ channels were without effect when applied to the cytosolic side of excised patches, such as internal tetraethylammonium or tetrapentylammonium (5 mM), or external charybdotoxin (10 nM) or apamin (10 nM), whereas quinidine in high concentrations (> 100 μM) produced a flicker-type block. In excised outside-out patches exposed to symmetrical K_{int} solutions, external Cs^+ caused a flicker-type block which increased with membrane hyperpolarization. Maximal inhibition was produced at 5 mM CsCl with an apparent K_i = 300 μM.

The K_{ir} channel is less permeant to Rb^+ and a permselectivity ratio P_{Rb}/P_K =

0.67 ± 0.04 (n = 6 patches) was calculated from changes in the reversal potential after equimolar substitution of KCl with RbCl.

Whole-Cell Recordings of K_{ir} Current

Whole-cell current was recorded from isolated single principal cells separated from neighboring cells by mechanical suction while incubated in calcium-free Ringer solutions. Under physiological ionic gradients (Na Ringer in bath, K_{int} pCa 8 solution in pipette), the whole-cell current displayed marked inward rectification. In kint solutions, the whole-cell currents exhibited time-dependent inactivation which was prevented when the pipette filling solution contained guanosine 5′-O-(3-thiotriphosphate) GTPγS (10 μM). We, therefore, routinely used GTPγS in whole-cell pipette filling solutions for the investigation of K_{ir} currents.

Fig. 10 *A* shows whole-cell currents generated at holding potentials between ±100 mV for cells bathed externally in 120 mM K^+, 54 mM K^+, and 3.7 mM K^+. The amplitude of inward current was increased at high external K^+ concentrations as expected for a K^+-selective membrane. The whole cell current records and the corresponding current–voltage relations in Fig. 10 *B*, illustrate the loss of outward K^+ current in high external K solutions which is a characteristic property of single K_{ir} channels. The whole-cell slope conductance for inward current greatly exceeds the conductance for outward current and changes in V_r produced by raising bath K^+ concentration agree with the predicted shift in E_K (Fig. 10 *C*). A slope of 56 mV/decade change in $[K]_o$ was calculated for the relationship V_r versus log $[K]_o$. Whole-cell currents are generated essentially by potassium flux through inward rectifier K^+ channels. The dependence of whole-cell conductance (for inward current) on external $[K^+]_o$ is shown in Fig. 11. The data were fit by a form of the Michaelis-Menten equation:

$$G_{cell} = \frac{G_{max} \cdot [K^+]_o}{[K^+]_o + [K^+]_{50}} \tag{12}$$

This analysis gave an upper limit for cell membrane conductance of 5,294 pS and a $[K^+]_{50}$ = 32 mM at which cellular conductance was half-maximal. A double logarithmic plot of G_{cell} versus $[K^+]_o$ had a slope of 0.59 which is close to the value expected (0.5) if conductance is proportional to the square root of $[K^+]_o$ as reported for inward rectifers in excitable cells (Hagiwara, 1983; Harvey and Ten Eick, 1988).

Whole-Cell Current Noise Analysis

The kinetics of K_{ir} channels and their contribution to the cell membrane conductance was further investigated by fluctuation noise analysis of whole-cell currents. Whole-cell membrane current noise was recorded at different external $[K^+]$ (3.7, 54, and 120 mM). The pipette solution contained K_{int} solution (pCa 8) with GTPγS (whole-cell solution in Table I). The power density spectra presented in Fig. 12 *A* were recorded at the Nernst potential for K and at holding potentials which generated electrochemical driving forces $\Delta\mu K$ = +90 or +100 mV favoring K^+ efflux and $\Delta\mu K$ = −90 or −100 mV driving K^+ influx. The power density spectra could be fit by a single Lorentzian function (solid line through the data points) which is indicative of

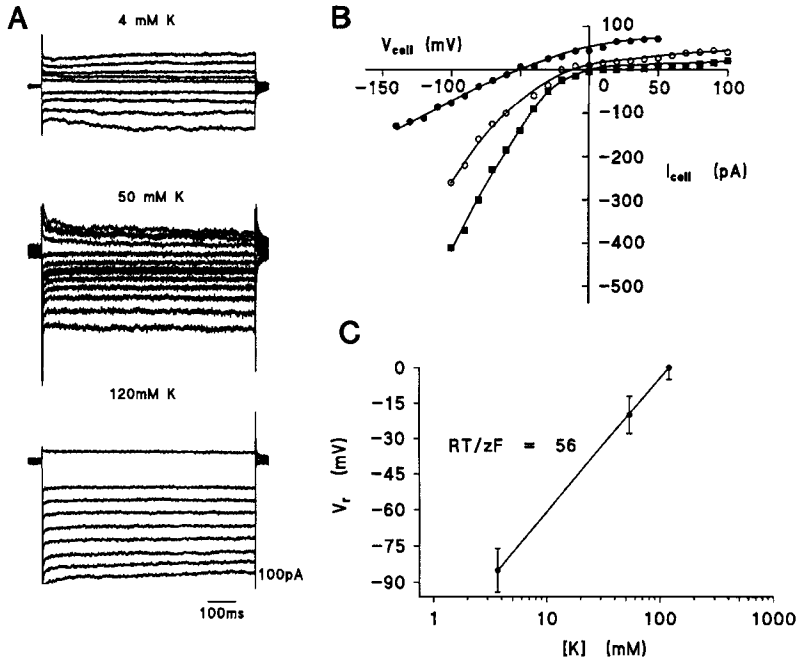

FIGURE 10. (A) Whole-cell current recordings as a function of external bath K^+ concentration (K_{int} solution in the pipette) in 120 mM K, 54 mM K, and 4 mM K. Negative (outward) currents were recorded at pipette potentials imposed in 10-mV steps to +100 mV. Positive (inward) currents were generated in increasing amplitude at pipette voltages clamped in 10-mV steps to −100 mV. Current signals were filtered at 5 kHz. Note disappearance of outward (negative) currents and increased amplitude of inward currents at raised external $[K^+]$. (*B*) Current–voltage relationship for the conditions 120 mM K (■), 54 mM K (○), and 3.7 mM K (●). In each case the current–voltage relation shows inward rectification and deviates from Goldman formalism. (*C*) The dependence of reversal potentials of whole-cell current on extracellular K^+ concentration (mean values for 12 cells at each different extracellular K concentration. The cell membrane behaves as a K^+ electrode.

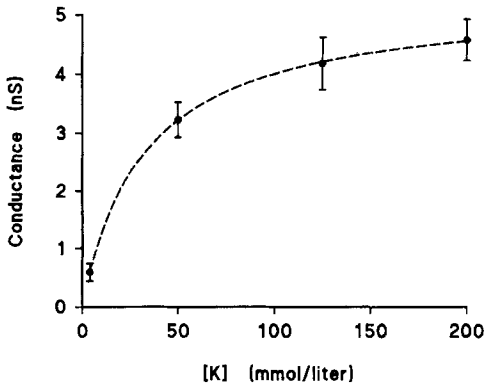

FIGURE 11. Whole-cell conductance for inward current plotted as a function of external potassium concentration ($n = 4$ cells). The solid line through the data points was drawn to Eq. 13 using values for G_{max} = 5.294 nS and $[K^+]_{50}$ = 32 mmol/liter.

an homogeneous population of spontaneously fluctuating channels. The results of the Lorenztian analysis for outward currents and inward currents at various extracellular K concentrations are summarized in Table II. The noise power decreased for outward currents and increased for inward current at high external [K]. This finding is in agreement with the K dependence of single channel and whole-cell currents. For example, cells exposed to physiological ion gradients at a holding potential of 15 mV ($\Delta\mu K = +100$ mV), the power density spectra of outward current fluctuations had a

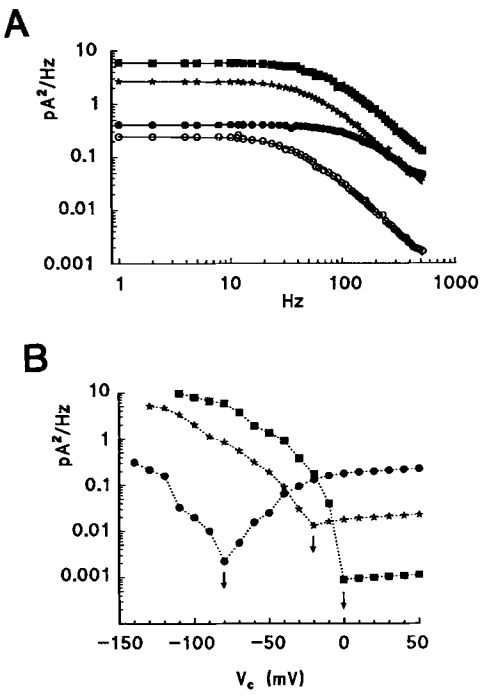

FIGURE 12. (*A*) Power density spectra (PDS) of fluctuations in whole-cell outward and inward currents as a function of applied voltage and external K^+ concentration (K_o)·(mean values for six cells at each K_o). The pipette was filled with K_{int} solution (Table I). The bath concentrations of K^+ and the electrochemical driving forces are given by the following symbols (■) K_o = 120 mM, $\Delta\mu K = -100$ mV. (★) K_o = 54 mM, $\Delta\mu K = -100$ mV. (●) K_o = 3.7 mM, $\Delta\mu K = -100$ mV. (○) K_o = 3.7 mM $\Delta\mu K = +100$ mV. The PDS were fit by a single Lorentzian function (solid line through data points) and a summary of data analysis is given in Table II. Raising external [K^+] increased the Lorentzian plateau and decreased the corner frequency for inward current fluctuations. Outward current noise power was greatly reduced in high K^+ solutions (not shown). No distinct Lorentzian could be discerned in the PDS when the patch membrane potential was clamped to the Nernst potential for K^+. (*B*). Voltage dependence of the plateau Lorentzian in the PDS of whole-cell current noise recorded under different external K^+ concentrations (mean values for six cells at each K_o). The pipette filling solution was K_{int} (120 mM K) throughout. The extracellular K^+ concentrations were as follows: (■) 120 mM K_o, (★) 54 mM K_o, (●) 3.7 mM K_o. In each case the minimum Lorentzian plateau value was measured at the K equilibrium potential (↓).

single corner frequency of 9 Hz and a Lorentzian plateau of 0.21 $pA^2 \cdot s^{-1}$. When the same cells were bathed in 54 mM K^+ the Lorentzian plateau was reduced 10-fold. Cells bathed in symmetrical K^+ solutions of 120 mM KCl, did not contain an evident corner frequency for outward current fluctuations.

The power density spectra of inward current noise fluctuations was also affected by varying external K^+ (Table II). The high corner frequency of inward current noise reflects rapid fluctuations between open and closed states which is a characteristic of

single K_{ir} channels. Calculations from noise analysis of single-channel open and closed times and conductance yielded values in agreement with the patch clamp data for single K_{ir} channels (Table II). For example, for inward current fluctuations recorded under physiological ionic gradients, the calculated off-rate $\alpha = 490\ s^{-1}$ (2 ms) is in excellent agreement with measured values for single K_{ir} channel mean open time = 3 ms. The equivalence between the mean open times obtained from single-channel recording and the off-rates determined from noise analysis demonstrates that the analyses are inherently consistent. Finally, the voltage dependence of the plateau Lorentzian (S_o) in the power density spectrum recorded at different extracellular K concentrations is shown in Fig. 12 *B*. The plateau Lorentzians show a minimum value at membrane potentials equal to the Nernst potential for K^+. For inward currents, the calculated number of active channels N increases with mem-

TABLE II

Lorentzian Analysis of Fluctuations of Outward and Inward Whole-Cell K^+ Currents as a Function of External $[K^+]$ (n = 8 cells for Each Different K Concentration)

	S_0	f_c	α	β	$*P_0$	G_S	I_S	N
	pA^2/Hz	*Hz*	s^{-1}			*pS*	*pA*	*channels/cell*
Outward currents								
3.7 mM K	0.21	9.0	1.55	55	0.97	5.2	0.7	109
($\Delta\mu K$ = 100 mV)	±0.07	±4.8	(3.1)					
54 mM K	0.027	16	78.5	22	0.22	1.4	0.31	41
($\Delta\mu K$ = 90 mV)	±0.005	±3	(100)					
Inward currents								
3.7 mM K	0.408	156	490	490	0.50	11.5	0.98	204
($\Delta\mu K$ = −85 mV)	±0.024	±20	(333)					
54 mM K	3.111	88	216	337	0.61	19.7	1.77	577
($\Delta\mu K$ = −90 mV)	±0.28	±16	(166)					
120 mM K	8.10	75	132	339	0.78	25	2.5	727
($\Delta\mu K$ = −100 mV)	±0.29	±6	(88)					

*Open probability was determined from excised inside-out patches under similar ionic gradients. Fluctuations in whole cell outward current at 120 mM extracellular K were of too low amplitude to give meaningful analysis. For comparison, the reciprocal of the measured single K_{ir} channel mean open time (off-rate) is given in parentheses under each α value.

brane hyperpolarization and extracellular K whereas the converse is true for outward currents. This phenomenon reflects the behavior of single K_{ir} channels to augment N in response to increasing extracellular K and hyperpolarization (compare Fig. 5 with Fig. 6 and Fig. 7 with Fig. 8). It is reasonable to conclude, therefore, that the whole-cell current noise is generated solely by fluctuations of a single population of inward-rectifier K^+ channels and the macroscopic membrane conductance is dominated by K_{ir} channel activity.

DISCUSSION

In the original Ussing model, the basolateral cell membrane conductance was portrayed as K^+ diffusion from the cell. Since then many microelectrode studies have

confirmed that potassium recycling across the basolateral membrane accounts for much of the total membrane conductance. The basolateral membrane behaves almost as a pure K^+ electrode in its potential response to changes in K^+ chemical gradient (Nagel, 1979). In this study, we have identified the type of K^+ channel normally present in the basolateral cell membrane of identified principal cells. The channel displays inward rectification under physiological ionic gradients and is the major determinant of membrane conductance. Our results from intact polarized epithelia can be compared to a recent patch clamp study of isolated frog skin cells which showed that most of the cell conductance is due to the activity of K^+ channels (García-Díaz, 1991). In the latter study ion channel activity was recorded in primary cultures of trypsin-isolated cells from *R. pipiens* and *R. catesbiana.* Inward rectification was a great deal less pronounced and single K^+ channel conductance was slightly larger (44 pS) in the cells studied by Garcia-Diaz compared to the diodelike inward rectification and single-channel conductance of 35 pS recorded in our experiments conducted with KCl Ringer (pCa 8) in the patch pipette. In experiments on trypsin-isolated cells from frog skin we have found the cell isolation procedure by itself can activate a calcium-dependent K^+ channel of 45 pS conductance (Harvey and Urbach, 1992). Inclusion of millimolar calcium in the patch pipette can also activate this channel at strong depolarizing potentials. This channel has a linear current–voltage relationship and is completely blocked by 100 μM quinidine. The presence of the ohmic K^+ channel in the Garcia-Diaz study would produce a masking of the inward rectifier and confer quinidine sensitivity to whole-cell K^+ currents. In our study on intact sodium-absorbing polarised epithelia, there is excellent agreement between the electrophysiological properties of the basolateral membranes of principal cells and single K_{ir} channels.

The property of anomolous rectification would seem to limit the usefulness of the K_{ir} channel to recycle K^+. However, under physiological conditions, the open probability is high for outward current over the normal range of membrane potentials. The low conductance of the K_{ir} channel for outward current would allow efficient voltage clamping of the membrane potential close to E_K with minimum loss of K^+ from the cell.

Comparison with Other Epithelial Inward-rectifier K Channels

Inward rectification of K^+ current is not a novel feature of epithelial cells and has been reported in macroscopic current–voltage relations for basolateral membranes of toad urinary bladder (Garty, 1984), frog skin (Nagel, 1985), and *Amphiuma* collecting tubule (Horisberger and Giebisch, 1988). Single-channel patch clamp data have revealed inward rectifier K channels in the basolateral membranes of dogfish rectal gland (Greger et al., 1987), and in basolateral membranes of renal tubule cells, *Necturus* proximal tubule (Kawahara, Hunter, and Giebisch, 1987), rabbit proximal tubule (Gogelein, Greger, and Schlatter, 1987; Parent, Cardinal, and Sauve, 1988), cultured MDCK cells (Ponce and Cereijido, 1991), and frog early distal tubule (Wang and Giebisch, 1989; Hunter, 1991). Inward rectifier K^+ channels are not confined solely to basolateral membranes but have also been reported in luminal membranes of MDCK (Friederich et al., 1989), cultured opossum (Ohno-Shosaku, Kubota, Yamaguchi, and Fujimoto, 1990), and rat collecting tubule (Frindt and Palmer, 1989;

Wang and Giebisch, 1989) and rabbit thick ascending limb of Henle's loop (Bleich, Schlatter, and Greger, 1990; Wang, White, Geibel, and Giebisch, 1990). Irrespective of their origin or localization, epithelial inward rectifier K^+ channels appear to share a common function; they are involved in moving K^+ out of the cell either as a net secretion (when present in the apical membrane) or K^+ recycling (when localized in the basolateral membrane) and as in frog skin principal cells, are the major determinant of membrane conductance.

The K_{ir} channel in frog skin epithelium presents some unusual features. Under physiological ion gradients, the single channel conductance increases with hyperpolarization but open probability increases with depolarization. This means that inward rectification cannot be ascribed to voltage dependence of channel activity ($N \cdot P_o$). Here we have shown that inward rectification results from block of outward current by cytosolic magnesium ions. The transformation of the K_{ir} channel to a pure inward rectifier in symmetrical K^+ solutions and the ohmic properties in Mg-free solutions under these conditions may indicate that Mg^{2+} inhibition of K_{ir} channels is potentiated by raising external $[K^+]$. Recently, it was shown that Mg^{2+} block of the K_{ir} channel in atrial muscle can be influenced by external K^+ (Matsuda, 1991).

The inhibition by external Ca^{2+} of inward currents in intact epithelia may explain the reduction of open probability with depolarization in calcium-containing external solutions. These results are similar to the observations of Ca^{2+} blockade of inwardly rectifying K^+ currents in guinea-pig ventricular myocytes (Biermans, Vereecke, and Carmeliet, 1987).

The anomolous rectifier properties of the K_{ir} channel may have a role in the kaliuretic response to hyperkalemia. The increased inward rectification in high K solutions would effectively reduce K^+ recycling across the basolateral membrane and thus favour net K^+ secretion. Conductance for inward whole-cell K_{ir} current increased proportionally with the square root of external K concentration whereas outward conductance decreased approximately fourfold at $[K^+]_o$ 3.7 to 10 mM. It would thus be expected that physiological changes in plasma $[K^+]$ of 2–8 mM which occur during adaptation of frogs and toads to high external KCl media will produce a marked reduction in K^+ recycling and facilitate K^+ secretion, as is observed under these conditions (Van Driessche and Zeiske, 1985).

E. Van Kerkhove was a visiting scientist supported by the Commissariat à l'Energie Atomique (CEA). The authors' research was funded by the Centre National de la Recherche Scientifique (URA 638) and the CEA (DB/SBCM) France.

Original version received 7 June 1993 and accepted version received 19 November 1993.

REFERENCES

Biermans, G., J. Vereecke, and E. Carmeliet. 1987. The mechanism of the inactivation of the inward-rectifying K current during hyperpolarizating steps in guinea-pig ventricular myocytes. *Pflügers Archiv.* 410:604–613.

Bleich, M., E. Schlatter, R. Greger. 1990. The luminal K^+ channel of the thick ascending limb of Henle's loop. *Pflügers Archiv.* 415:449–460.

Chang, D., and D. C. Dawson. 1988. Digitonin permeabilized colonic cell layers. *Journal of General Physiology.* 92:281–306.

Chang, D., P. S. Hsieh, and D. C. Dawson. 1988. Calcium: a program in BASIC for calculating the composition of solutions with specified free concentrations od calcium, magnesium and other divalent cations. *Computers in Biology and Medicine.* 18:351–366.

Farquhar, M. G., and G. E. Palade. 1965. Cell junctions in amphibian skin. *Journal of Cell Biology.* 26:263–291.

Friederich, F., H. Weiss, M. Paulmichl, and F. Lang. 1989. Activation of potassium channels in renal epitheliod cells (MDCK) by extracellular ATP. *American Journal of Physiology.* 256:C1016–C1021.

Frindt, G., and L. G. Palmer. 1989. Low conductance K channels in apical membrane of rat cortical collecting tubule. *American Journal of Physiology.* 256:F143–F151.

García-Díaz, J. F. 1991. Whole-cell and single channel K^+ and Cl^- currents in epithelial cells of frog skin. *Journal of General Physiology.* 98:131–161.

Garty, H. 1984. Current–voltage relations of basolateral membrane in tight amphibian epithelia: use of nystatin to depolarize the apical membrane. *Journal of Membrane Biology.* 77:213–222.

Gögelein, H., R. Greger, and E. Schlatter. 1987. Potassium channels in basolateral membrane of the rectal gland of Squalus acanthias. *Pflügers Archiv.* 409:107–113.

Greger, R., H. Gögelein, and E. Schlatter. 1987. Potassium channels in the basolateral membrane of the rectal gland of the dogfish (Squalus acanthias). *Pflügers Archiv.* 409:100–106.

Hagiwara, S. 1983. Membrane Potential-dependent Ion Channels in Cell Membrane. Raven Press, New York. 65–78.

Hamill, O. P., A. Marty, E. Neher, B. Sakmann, and F. Sigworth. 1981. Improved patch-clamp techniques for high resolution recording from cells and cell-free membrane patches. *Pflügers Archiv.* 391:85–100.

Harvey, B. J., and R. P. Kernan. 1984. Intracellular ionic activities in relation to external sodium and effects of amiloride and/or ouabain. *Journal of Physiology.* 349:501–517.

Harvey, B. J., S. R. Thomas, and J. Ehrenfeld. 1988. Intracellular pH controls cell membrane Na^+ and K^+ conductances and transport in frog skin epithelium. *Journal of General Physiology.* 92:767–791.

Harvey, R. D., and R. E. Ten Eick. 1988. Characterization of the inward rectifying potassium current in rat ventricular myocytes. *Journal of General Physiology.* 91:593–615.

Harvey, B.J., and V. Urbach. 1992. Cellular regulation of ATP and calcium-sensitive K^+ channels in frog skin and distal renal cell culture A6 epithelia. *Journal of General Physiology.* 100:18*a*. (Abstr.)

Horisberger, J.-D., and G. Giebisch. 1988. Voltage dependence of basolateral membrane in the Amphiuma collecting tubule. *Journal of Membrane Biology.* 105:257–263.

Hunter, M. 1991. Potassium selective channels in the basolateral membrane of single proximal tubule cells of frog kidney. *Pflügers Archiv.* 418:26–34.

Kawahara, K., M. Hunter, G. Giebisch. 1987. Potassium channels in *Necturus* proximal tubule. *American Journal of Physiology.* 253:F488–F494.

Koefoed-Johnsen, V., and H. H. Ussing. 1958. The nature of the frog skin potential. *Acta Physiologica Scandinavica.* 42:293–308.

Kristensen, P., and H. H. Ussing. 1985. Epithelial organization. *In* The Kidney: Physiology and Pathophysiology. D. W. Seldin and G. Giebisch, editors. Raven Press, New York. 173–188.

Matsuda, H. 1991. Effects of external and internal K^+ ions on magnesium block of inwardly rectifying K^+ channels in guinea pig heart cells. *Journal of Physiology.* 435:83–99.

Nagel, W. 1979. Inhibition of potassium conductance by barium in frog skin epithelium. *Biochimica et Biophysica Acta.* 55:346–357.

Nagel, W. 1985. Basolateral membrane ionic conductance in frog skin. *Pflügers Archiv.* 405(Suppl. 1):S39–S43.

Ohno-Shosaku, T., T. Kubota, J. Yamaguchi, and M. Fujimoto. 1990. Regulation of inwardly rectifying K^+ channels by intracellular pH in opossum kidney cells. *Pflügers Archiv.* 416:138–143.

Parent, L., J. Cardinal, and R. Sauve. 1988. Single channels analysis of a K channel at basolateral membrane of rabbit proximal convoluted tubule. *American Journal of Physiology.* 254:F105–F113.

Ponce, A., and M. Cereijido. 1991. Polarized distribution of cation channels in epithelial cells. *Cellular physiology and Biochemistry.* 1:13–23.

Rick, R., A. Dorge, E. von Arnim, and K. Thurau. 1978. Electron microprobe analysis of frog skin epithelium: evidence for a syncitial sodium transport compartement. *Journal of Membrane Biology.* 39:313–331.

Sharin, S. H., and J. T. Blankemeyer. 1989. Demonstration of gap junctions in frog skin epithelium. *American Journal of Physiology.* 257:C658–C664.

Van Driessche, W., and W. Zeiske. 1985. Ionic channels in epithelial cells. *Physiological Reviews.* 65:833–903.

Wang, W., and G. Giebisch. 1991. Dual effect of ATP on the apical small conductance potassium channel of the rat cortical collecting duct. *Journal of General Physiology.* 98:35–62.

Wang, W., S. White, J. Geibel, and G. Giebisch. 1990. A potassium channel in the apical membrane of rabbit thick ascending limb of Henle's loop. *American Journal of Physiology.* 258:F244–F253.